Development of Eye-Safe Fiber Lasers Near 2 μm

Jihong Geng, Qing Wang, Yinwen Lee, and Shibin Jiang

(Invited Paper)

***Abstract*—Eye-safe fiber laser sources near 2 μm have attracted a lot of interest in space, defense, medical, and industrial applications. We review our latest developments of various fiber laser sources operating near 2 μm, which include single-frequency CW lasers, wavelength-swept lasers, power-scaled nanosecond pulsed lasers, and various mode-locked lasers. Potential applications of these mid-infrared fiber laser sources are also discussed.**

***Index Terms*—Mode-locked fiber laser, silicate glass, single-frequency fiber laser, Tm-doped fiber, Tm-Ho-codoped fiber, tunable fiber laser, Q-switched fiber laser.**

I. Introduction

LASER EMISSIONS near 2 μm based on Tm^{3+} and Ho^{3+} ions have attracted intense interest in recent decades for a number of potential applications, including atmospheric measurements, laser radar, longer-wavelength laser pumping, laser plastics material processing, biomedical and medical applications (such as laser angioplasty, ophthalmic procedures, laser lithotripsy, and laser surgeries). The Tm^{3+} and Ho^{3+} ions can be doped in many laser host materials, including crystals, various oxide glasses (such as silica, silicate, germanate, and tellurite), fluoride glasses, and chalcogenide glasses. Those Tm^{3+} and Ho^{3+} doped glass materials are of particular interest, because they enable fiber-based laser operations in the 2-μm spectral region. Performance of a fiber-based laser can be superior to that of its bulk crystalline laser counterparts in many aspects, including compactness, robustness, long-term reliability, better thermal management, and high beam quality at high average powers [1]. Therefore, Tm^{3+} and Ho^{3+} doped fiber lasers have been extensively investigated in the recent two decades.

The Tm^{3+} and Ho^{3+} ions doped in glass/fiber materials, exhibit wide and gain bandwidths covering from 1.7 μm to 2.1 μm. The wide gain bandwidth provides a wide selection range of laser operation wavelengths in the eye-safe spectral region when operating in continuous-wave (CW) mode or Q-switched mode. It can also offer the capability of delivering femtosecond laser pulses when operating in a mode-locking regime. These laser operation modes have been demonstrated in a Tm^{3+} and/or Ho^{3+} doped fiber laser with different host materials.

Manuscript received December 21, 2013; revised February 14, 2014, April 4, 2014 and April 10, 2014; accepted April 11, 2014. Date of publication April 21, 2014; date of current version June 2, 2014. This work was supported by NASA, NIST, U.S. Air Force, and U.S. Department of Energy.

J. Geng, Q. Wang, and S. Jiang are with AdValue Photonics, Tucson, AZ 85714 USA (e-mail: jgeng@ advaluephotonics.com; qwang@ advaluephotonics.com; sjiang@advaluephotonics.com).

Y. Lee is with the Department of Electro-optical Engineering, National Taipei University of Technology, Taipei 10608, Taiwan (e-mail: ywlee@ntut.edu.tw).

Color versions of one or more of the figures in this paper are available online at http://ieeexplore.ieee.org.

Digital Object Identifier 10.1109/JSTQE.2014.2318274

Because the spectral region contains many absorption lines of important atmospheric gases such as H_2O and CO_2, CW and pulsed single-frequency 2-μm laser sources have been widely used in atmospheric remote sensing applications especially for coherent Doppler lidar wind detection [2], [3]. A highly-reliable single-frequency fiber laser provides an ideal robust fiber seed source for those applications, for which one popular wavelength region is 2.05–2.06 μm. At that wavelength, high-energy Ho:Tm:YLF and Ho:YLF crystal-based power amplifiers have been demonstrated with joule-level energy of single-frequency laser pulses.

The nature of high absorption near the 2-μm spectral region in liquid water [4] and most polycarbonate materials makes the Tm^{3+} and/or Ho^{3+} doped laser sources attractive in many industrial applications, such as biomedical/medical applications, and plastics material processing. Both CW and pulsed 2-μm fiber lasers can find their applications in those industrial areas.

One popular military application for 2-μm lasers is to use them as pump sources for longer wavelength mid-infrared generation via nonlinear frequency conversion, such as optical parametric oscillator (OPO) [5]. Nonlinear frequency conversion processes prefer high-peak-power pulsed lasers, including Q-switched and/or mode-locked lasers. Pulsed 2-μm lasers are more favorable to be used as pump sources for longer wavelength infrared generation for some reasons, as compared with those counterparts at the wavelengths of 1 μm and 1.55 μm. First, it has a lower quantum defect for the frequency conversion from pump wavelength to mid-infrared signal wavelengths, thereby yielding higher quantum efficiency in the nonlinear process. Second, many nonlinear optical crystals for mid-infrared generation are not transparent or have a high propagation loss at the shorter pump wavelengths. Third, for some nonlinear optical crystals with too large dispersion, even no phase-matching can be obtained for OPO nonlinear process when the pump wavelength is short (e.g., 1 μm).

Another emerging application for 2-μm lasers is for mid-infrared supercontinuum generation. Mid-infrared broadband radiation is very useful for a variety of applications. Supercontinuum generation in a piece of highly nonlinear passive fiber is a commonly-used way to obtain broadband laser radiation, through various nonlinear optical effects in the nonlinear fiber when pumping with a high-power pulsed or even CW laser. These nonlinear effects include self-phase modulation (SPM), Raman scattering, modulation-instability, and so on [6]. To enhance the efficiency and the bandwidth of supercontinuum generation, dispersion-engineered nonlinear fibers (such as microstructured fiber or fiber taper) are usually used, so that the pump lasers can propagate in those dispersion-engineered nonlinear fibers in an anomalous dispersion regime. This requires the pump laser wavelength be close to or longer than zero-dispersion wavelengths (ZDW) of the nonlinear fibers. Also,

to obtain efficient mid-infrared supercontinuum generation, the nonlinear fiber must have low propagation loss at both pump wavelength and supercontinuum wavelengths. The best-known infrared transparent fibers are made of non-silica soft glasses, including fluoride glass and chalcogenide glasses. The challenge is these soft glasses exhibit longer ZDW [7]. Some chalcogenide glasses even are not transparent at short wavelengths, such as 1 μm and 1.55 μm. Therefore, 2-μm laser sources are favorable pump sources for mid-infrared supercontinuum generation.

In this paper, we present our development of various 2-μm fiber lasers [8]. This paper is structured as follows. Section II describes heavily $Tm^{3+}-$ and/or $Ho^{3+}-$doped silicate glass fibers that we used to develop various 2-μm fiber lasers. Section III$\sim$VI describes what we did with single-frequency 2-μm fiber lasers, tunable 2-μm fiber laser, Q-switched 2-μm fiber lasers, and mode-locked 2-μm fiber lasers.

II. Heavily Tm- and Ho-Doped Silicate Glass Fiber

So far, many different glass host materials have been used to fabricate Tm^{3+}- and/or Ho^{3+}-doped fiber for 2-μm laser operation, including silica and non-silica oxide glass fiber such as germanate [9] and telluride glass fiber [10]. It is well known that the doping concentration of rare-earth ions in silica fiber is limited due to the intrinsic glass network structure. Various approaches are developed to increase the doping concentration including co-doping with Al_2O_3, B_2O_3, and P_2O_5 and using nano-particle technology. The highest doping level in silica glass has been increased to 1 or 2-wt%. In recent years, particularly, dramatic improvements in Tm^{3+}-doped silica fiber technology (by codoping some other ions such as Ge^{4+} and Al^{3+} in silica glass of the fiber core during the chemical vapor deposition process) have led to successful demonstrations of very high laser efficiency (>54%) with 1-kW laser average power near 2 μm.

Multi-component non-silica glasses permit a higher doping concentration of Tm^{3+} ions, due to their less-defined glass network as compared to silica glass. Various multi-component glass fibers have been demonstrated for 2-μm laser operation, including silicate, germanate, and tellurite glass fiber. These multi-component glass fibers with high doping concentration of Tm^{3+} ions allow for taking the advantage of a 2-for-1 cross-relaxation process in the heavily Tm^{3+} doped systems, yielding even higher laser efficiency than silica doped glass fiber. More than 100-W laser output has been demonstrated in a germanate glass fiber laser with 5-wt% Tm^{3+} doping concentration. More importantly, high doping concentration fiber also enables high pump absorption and high gain per unit length, which is particularly essential for some applications that need high laser gain generated from a short piece of active fiber. However, it is noted that these important benefits come from multi-component non-silica glass fibers at some expenses, such as weak mechanical strength and the difficulty in fusion splicing with silica fiber pigtails of commercial fiber components.

We fabricated multi-component silicate glasses with Tm_2O_3 doping concentration from 4 to 7-wt%. The main glass network that forms our glass host is SiO_2, the same material as standard silica glass fiber. Therefore, silicate glass fibers provide much stronger mechanical strength than other multi-component glass fibers, and better compatibility with silica fiber, yielding much more robust fusion splicing between active fiber and standard passive silica fiber that is needed to build fiber lasers/amplifiers, such as fiber Bragg gratings or pump combiners.

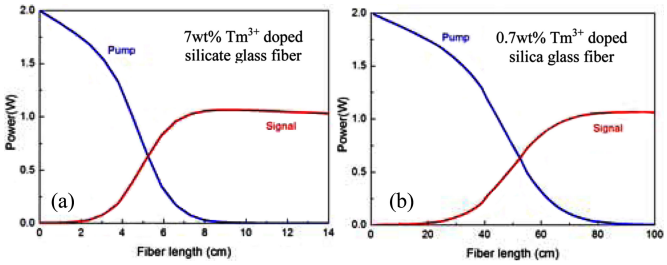

Fig. 1. Calculated output signal and residual pump powers of 1950 nm Tm^{3+}-doped fiber amplifier as a function of the fiber length. (a) 7-wt% Tm^{3+}-doped silicate fiber; (b) 0.7-wt% Tm^{3+}-doped silica fiber. Signal power is 1 mW. The pump is 2-W 1575 nm laser.

As mentioned above, one of the most important benefits of multi-component glass fibers is high pump absorption and high gain per unit length. In order to compare the optical difference between multi-component glass fibers and a silica glass fiber. We have numerically analyzed optical performance of a fiber amplifier with two different Tm^{3+}-doped fibers. One fiber is one of our Tm^{3+}-doped silicate fibers, and the other one is a Tm^{3+}-doped silica fiber. It was assumed that both fibers have the same design and both fiber amplifiers have the same configuration, only with different fiber lengths. The amplifier is seeded with a 1950-nm laser signal at 1 mW, and pumped by a 1575-nm pump laser at 2 W. Both active fibers are taken to have a single-mode core diameter of 10 μm and a cladding diameter of 125 μm. To reflect actual differences between the two types of fibers, namely their propagation loss, upper-state lifetime, and Tm^{3+} concentration, each of these three parameters is given its actual measured value for each fiber. For the silica fiber, we used the best values currently reported for commercial fibers, i.e., a loss of 0.1 dB/m, an upper-state lifetime of 0.65 ms, and a concentration of $8.4 \times 10^{19} Tm^{3+} ions/cm^3$ [11]. The corresponding values for our silicate fiber (7-wt% Tm^{3+} doping) are 0.7 dB/m, 0.635 ms, and $8.35 \times 10^{20} Tm^{3+} ions/cm^3$, respectively. We used the measured absorption and emission cross-section spectra of these two glasses as the calculation input. The calculated results are shown in Fig. 1. It is obvious that high laser gain can be generated from our heavily doped silicate glass fiber in a much shorter fiber length. This feature particularly benefits the applications that require high laser gain generated from a short piece of active fiber, such as short-cavity single-frequency laser operation and high-power pulsed fiber amplifiers (for Brillouin scattering suppression).

Fig. 2 shows typical microscopic images of some heavily Tm^{3+}- and/or Ho^{3+}-doped silicate glass fibers. Both single-cladding and double-cladding silicate glass fiber can be fabricated in house by using the well-known rod-in-tube fiber drawing technique. For double-cladding fibers, the inner cladding is surrounded by a layer of outer cladding silicate glass with NA as large as $\sim$0.6 to confine the multimode pump laser in the inner cladding region. The use of glass outer-cladding in the fibers allows potentially for much higher power handling capability than those standard polymer-based double-cladding

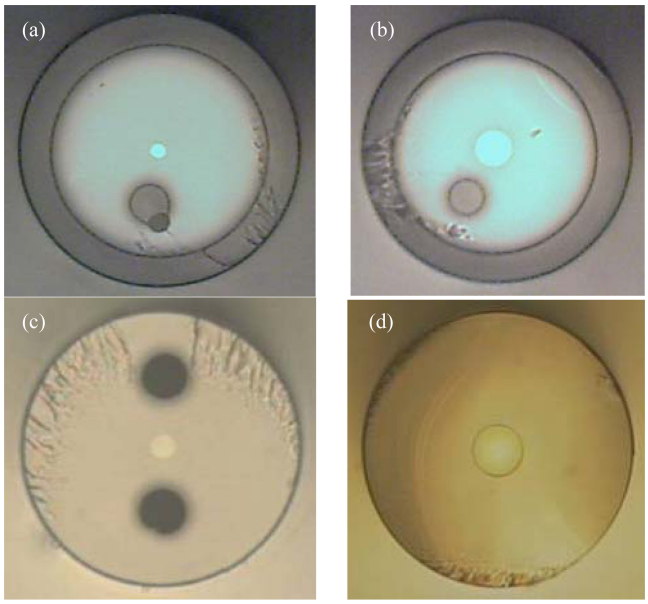

Fig. 2. In-house-fabricated Tm^{3+}- and/or Ho^{3+}-doped silicate glass fibers. (a) double-cladding single-mode fiber. (b) double-cladding LMA fiber. (c) single-cladding polarization-maintaining fiber. (d) single-cladding LMA fiber.

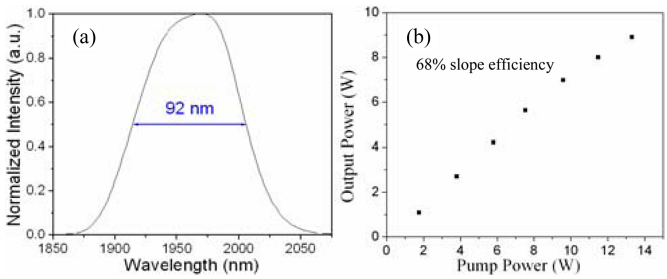

Fig. 3. (a) ASE spectrum of in-house-fabricated cladding-pumped Tm^{3+}-doped silicate glass fiber (5wt% Tm^{3+}). (b) Laser output power as a function of absorbed pump power at 798 nm in cladding-pumped Tm^{3+}-doped fiber laser at 1.95μm with 20-cm-long 18 μm core fiber.

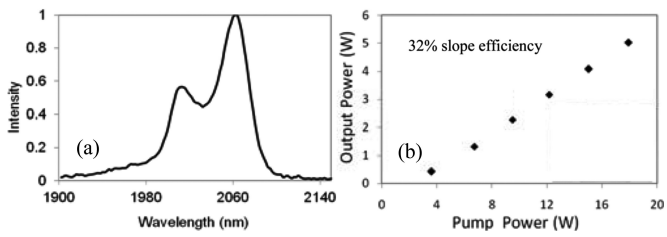

Fig. 4. (a) ASE spectrum of in-house-fabricated cladding-pumped Tm^{3+}-Ho^{3+}-codoped silicate glass fiber (6wt% Tm^{3+} and 0.4wt% Ho^{3+}). (b) Laser output power as a function of absorbed pump power at 798nm in cladding-pumped co-doped fiber laser at 2.06 μm with 120 cm-long 11 μm core fiber.

silica fibers. A low-index silicate rod is usually inserted into the inner cladding for the enhancement of cladding pump absorption (>12 dB/m near 800 nm). In a similar way, we are also able to fabricate single-cladding polarization-maintaining (or non-PM) heavily Tm^{3+}-doped silicate glass fiber.

Fig. 3 and Fig. 4 show typical amplified spontaneous emission (ASE) spectra of in-house Tm^{3+}-doped and Tm^{3+} -Ho^{3+}-codoped silicate glass fibers, and their laser performances of cladding-pumped laser operation using these silicate fibers. High-gain per unit length associated with our heavily doped silicate glass fibers enables us to develop various unique fiber lasers near 2 μm, including CW single-frequency fiber lasers and high-power pulsed fiber lasers.

III. Single-Frequency Fiber Laser Near 2 μm

Advances in the development of single-frequency narrow-linewidth fiber lasers are beneficial to a variety of applications. Single-frequency fiber lasers at 1 μm and 1.55 μm have been well developed and commercialized with a typical design of a very short laser cavity in combination with narrow-band fiber Bragg gratings for robust single-frequency operation. Similar laser development near 2 μm has received intense interests in recent years. Single-frequency pulsed laser sources in the eye-safe spectral region near 2 μm are of particular interest to some applications. For example, Doppler lidar wind measurements require highly reliable compact single-frequency laser pulses near 2 μm for use in airborne and space-borne platforms. Another emerging application is to use single-frequency pulsed 2 μm lasers as pump sources for narrowband longer wavelength infrared or THz generation via nonlinear frequency conversion techniques, such as OPO or difference frequency generation.

To date, two different kinds of Tm-doped glass fibers have been used for single-frequency laser operation near 2 μm. They are silica glass fiber with distributed feedback (DFB) cavity configuration [12]–[15] and non-silica glass fiber with distributed Bragg reflector (DBR) configuration [16]. The DBR fiber laser technology provides much more flexibility in the wavelength of a single-frequency fiber laser.

High pump absorption and high gain per unit length of heavily doped multi-component non-silica glass fibers make it possible for achieving efficient single-frequency laser operation from a short-cavity DBR fiber laser at any wavelength in the whole gain spectral region. Usually, a single-frequency DBR fiber laser is built by using a short piece of heavily doped active fiber and a pair of fiber Bragg gratings that are written in commercial single-mode fibers.

A. Tm-Doped Single-Frequency Fiber Laser

Both Tm^{3+} and Ho^{3+} ions exhibit high laser gain near 2 μm when they are doped in optical media, including crystals and various glass fibers. To date, Tm^{3+}-doped fiber lasers have dominated research interest in the 2-μm fiber lasers. Indeed, Tm-doped fibers have the potential to generate laser wavelengths far beyond 2.0 μm, up to 2.1 μm, which covers the most of gain spectral range offered by Ho^{3+}-doped fibers. However, for single-frequency laser operation Tm^{3+}-doped fibers cannot go that far. This is because the emission cross section of Tm^{3+} ions is dramatically reduced with increased wavelength (beyond 2 μm). For laser operation at the wavelengths far beyond 2 μm, a prolonged length of Tm^{3+}-doped gain fiber has to be used to generate sufficient laser gain, which is prohibited for single-frequency laser operation. The reported longest single-frequency laser wavelength so far from a Tm^{3+}-doped fiber laser was near 2.02 μm [16]. With a short piece of heavily Tm^{3+}-doped non-silica fiber and a DBR cavity configuration

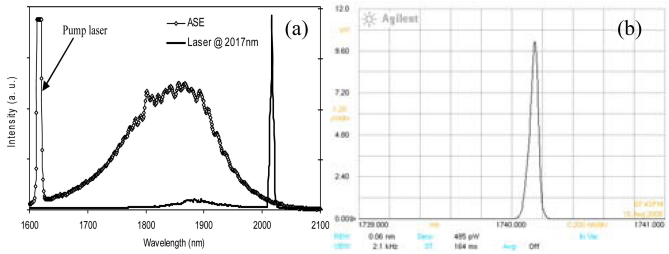

Fig. 5. Single-frequency laser operation at (a) 2017nm and (b) 1740nm from a Tm^{3+}-doped DBR fiber laser. (Copied from [16].)

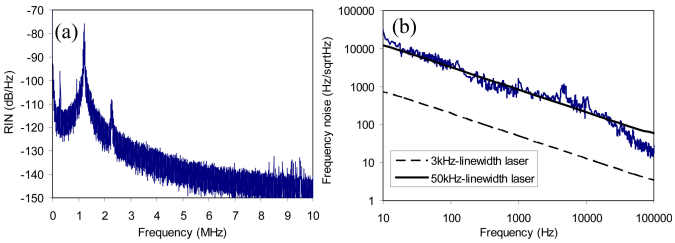

Fig. 6. (a) Typical RIN spectrum and (b) frequency noise spectrum of a single-frequency DBR fiber laser near 2 μm.

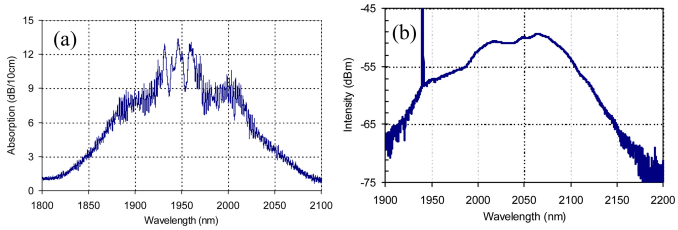

Fig. 7. (a) Absorption spectrum and (b) ASE spectrum measured with a 10-cm-long piece of single-mode 3-wt% Ho-doped silicate glass fiber. A pump laser line at 1940 nm appears in the right graph.

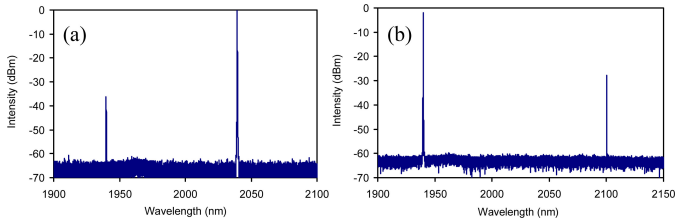

Fig. 8. Optical spectra of single-frequency fiber lasers at (a) 2040 nm and (b) 2100 nm with 2-cm long Ho-doped fiber (and its pump laser line at 1940 nm).

pumped by a single-mode laser beam at 793 nm, germanate glass active fiber has been successfully used for building single-frequency fiber lasers in a wide wavelength range, for example from 1740 to 2020 nm, as shown in Fig. 5.

Fig. 6 shows typical noise spectra of a single-frequency Tm^{3+}-doped fiber laser. The laser features a relaxation-oscillation-dominated relative intensity noise (RIN) peak (-75 dB/Hz) at $\sim$1 MHz and a spectral linewidth of $\sim$50 kHz. The output power can be 10s of mW directly obtained from a fiber laser oscillator [31], and the power can be readily scaled up to 5W or more with Brillouin-suppressed fiber amplifiers.

B. Ho-Doped Single-Frequency Fiber Laser

Some applications need the operation wavelength of a single-frequency laser longer than 2.02 μm. For atmospheric Doppler lidar application, for instance, one popular wavelength region is 2.05–2.06 μm, at which high-energy Ho:Tm:YLF and Ho:YLF crystal-based power amplifiers are readily available for joule-level pulse energy single-frequency laser generation. In this application, it requires single-frequency seeder laser at the wavelength near 2.05–2.06 μm. This is a challenge if using Tm-doped fibers, but it is readily achievable with Ho^{3+}-doped fibers. In fact, Wu demonstrated the first single-frequency fiber laser at that wavelength by using heavily Ho-doped germanate glass fiber [18].

Recently, we have also demonstrated a single-frequency fiber laser using a very short piece of heavily Ho^{3+}-doped silicate glass fiber, as described in detail in [19]. The single-mode Ho^{3+}-doped fiber has a doping concentration of 3wt% with a core diameter of 10 μm and 0.124 NA.

Fig. 7(a) shows absorption spectrum of a 10-cm-long piece of the 3wt% Ho^{3+}-doped fiber. For the Ho^{3+}-doped fiber, the absorption is high ($\sim$1.2 dB/cm) at the center absorption wavelength near 1.95 μm, which enables us to use a very short piece ($\sim$2-cm long) of the Ho^{3+}-doped fiber as the gain fiber for single-frequency laser operation when pumped with a 1.95 μm Tm^{3+}-doped laser. Fig. 7(b) also shows ASE spectrum from the fiber when pumped by a fiber laser at 1940 nm, exhibiting a wide gain spectrum.

In order to demonstrate the capability of the Ho^{3+}-doped fiber for single-frequency laser operation in a wide spectral range, we used a short piece ($\sim$2-cm long) of the 3-wt% Ho^{3+}-doped fiber as the gain fiber, and two pairs of fiber Bragg gratings at 2.04 μm and 2.1 μm to form a monolithic DBR laser cavity. We successfully obtained laser oscillation at both wavelengths, as shown in Fig. 8. This demonstration indicates that the gain of the Ho-doped fiber was sufficiently high for single-frequency laser operation at any wavelength in a wide spectral range from 2.04 μm up to 2.1 μm.

IV. All-Fiber Wavelength-Swept Laser Near 2 μM

Broad wavelength tunability of a Tm-doped fiber laser has been reported for two decades [20]. However, previous demonstrations use fragile free-space laser cavity designs in those Tm-doped fiber lasers. All-fiber wavelength-swept fiber lasers have been demonstrated with both Tm^{3+}- and Ho^{3+}-doped fibers. The laser wavelength can be rapidly swept over a wide spectral range by using a fiber Fabry-Perot tunable filter (FFP-TF). This kind of fiber laser has been demonstrated in 1-μm and 1.55-μm wavelength regions previously [21], [22], but never in the 2-μm wavelength region.

The key component in the all-fiber tunable laser was a fiber-based FFP-TF that was fabricated for the operation at 2 μm by Micron Optics [23]. High-reflectivity thin-film coating on the two fiber ends to form a high finesse cavity (finesse $\sim$ 2300). A piezo actuator was bonded with the FP filter for achieving fast wavelength tuning.

The all-fiber wavelength-swept laser was be built by inserting a fiber-based tunable filter into a Tm^{3+}- or Ho^{3+}-doped fiber ring cavity. For Tm^{3+}-doped fiber, a CW single-mode Er-doped

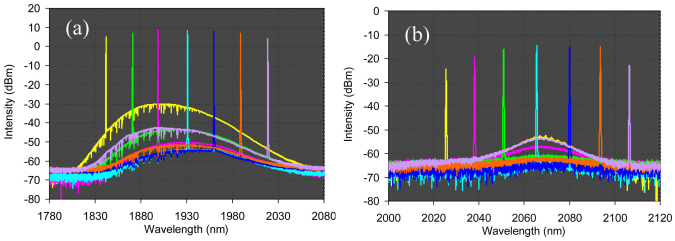

Fig. 9. Typical laser spectra of the all-fiber wavelength-swept fiber lasers with (a) Tm^{3+}-doped fiber and (b) Ho^{3+}-doped fiber when constant voltages were applied to the tunable filter.

fiber source at 1.56 μm, which was a home-made Er-doped fiber laser cladding-pumped by a commercial fiber-pigtailed 960-nm single emitter, was used as a pump source via a fiber wavelength-division multiplexer (WDM) for the wavelength at 1.5 μm/2.0 μm, which was detailed in [23]. For Ho^{3+}-doped fiber, similarly, a CW single-mode Tm^{3+}-doped fiber source at 1.95 μm was used as a pump source via a fiber WDM for the wavelength at 1.95 μm /2.05 μm. All of the intracavity components, including an isolator, the tunable filter, and a 50/50 splitter, were fusion-spliced together to form an all-fiber laser ring cavity.

Fig. 9 shows typical laser spectra when constant voltages were applied to the filter. Laser wavelength was determined by transmission wavelength of the tunable filter, which in turn was piezo-electrically controlled by the voltage that was applied to the filter. With a 50-cm-long Tm^{3+}-doped fiber, the laser wavelength can be tuned over 200 nm from 1840 to 2040 nm. For Ho^{3+}-doped fiber, the laser wavelength can be tuned over 80 nm from 2025 to 2105 nm.

When a sawtooth voltage was applied to the filter, the laser wavelength can be linearly swept rapidly. The laser wavelength was swept over the whole spectral range in just about 16ms, at a speed of about 10 μm/sec [23].

Spectral linewidth of the laser was measured by using a high-resolution scanning fiber Fabry-Perot (FP) interferometer (Micron Optics, FSR = 1GHz, finesse ~270). The measured spectral linewidth was about ~300 MHz, or $0.01\ cm^{-1}$ [23]. The narrow-linewidth tunable laser can be used for high-resolution spectroscopic measurements.

V. All-Fiber Q-Switched Fiber Laser Near 2 μm

In the past decade, pulsed fiber lasers have been extensively investigated due to their superior performances for military and industrial applications, such as LIDAR sensing, nonlinear frequency conversion, and material processing. Most pulsed fiber lasers demonstrated so far are based on Yb- and Er-doped fibers. Mille-joule-level nanosecond pulsed fiber lasers at 1 μm have been well-commercialized for material processing applications, such as marking, trimming, drilling, and cutting. Pulsed fiber lasers operating near 2 μm are emerging laser sources for scientific and industrial applications, because of their unique advantages in terms of eye-safe wavelength, and high absorption in greenhouse gases, liquid water, and most polycarbonate materials. Potential applications with 2-μm pulsed fiber lasers include eye-safe LIDAR, medicine, spectroscopy, remote sensing, and pumping source of mid-infrared generation.

Both Q-switching and gain switching techniques have been used to generate nanosecond fiber laser pulses near 2 μm. The Q-switching technique includes active Q-switching with acousto-optic modulator [24] and passive Q-switching with saturable absorber materials, such as Cr^{2+}:ZnSe [25], Ho^{3+}-doped fiber [26], and Sb-based semiconductor saturable absorber [27]. Direct gain switching can be realized by pumping with either a modulated 1.55-μm laser [28] or a pulsed laser at 1.9 μm [29]. So far, the highest peak power reported from a 2-μm fiber laser system is 138 kW with a pulse energy over 10 mJ [29], which was achieved by using a Tm:YLF crystal-based pumping source.

Some applications (e.g., coherent lidar sensing for wind measurement or CO_2 profiling in the atmosphere) require a 2-μm laser not only in a pulsed mode, but also in single-frequency mode. For decades, Q-switched single-frequency Tm^{3+}- or Ho^{3+}-doped crystal lasers have been used in these applications [2], although they suffer from a complicated free-space laser cavity design. All-fiber monolithic laser sources are highly desirable for these applications, especially for airborne and space-borne applications, because fiber-based sources offer a much more compact and robust solution. With the advances in photonic component technologies developed mainly for telecommunication and fiber laser industries in recent years, all-fiber single-frequency pulsed laser sources become readily available at shorter wavelengths, i.e., 1.55 μm and 1 μm as well. High-power single-frequency pulse radiation can simply be generated from directly-modulated DFB semiconductor laser and/or single-frequency fiber oscillators in combination with fiber- or crystal-based high power amplifiers. For the long wavelengths near 2 μm, fiber components are not as readily available as those at the short wavelengths (1.55 μm and 1 μm). Although single-frequency DFB diodes near the 2-μm band become available in recent years, the accessible wavelengths of 2-μm-band DFB laser diodes are quite limited, not to mention their wavelength accuracy and stability.

High laser gain per unit length associated with our heavily doped silicate glass fibers make it possible for us to develop all-fiber pulsed single-frequency lasers. It also benefits our development of high-power pulsed fiber amplifiers from mitigating the limit of nonlinear effects in the amplifiers.

A. All-Fiber Q-Switched Single-Frequency Tm-Doped Laser

The approach for an all-fiber Q-switched single-frequency laser is based on polarization modulation of a short-cavity fiber laser by using stress-induced birefringence [30], as illustrated in Fig. 10. As described with more details in [17], the design concept is that a single-frequency DBR fiber laser is formed by a non-polarization-maintaining (non-PM) high-reflectivity fiber Bragg grating (FBG) as the cavity end mirror and a polarization-maintaining (PM) narrow-band FBG that acts as an output coupler. The combined use of a short laser cavity (a few centimeters in length) and narrow-band distributed Bragg reflectors (i.e., FBGs) ensures robust single-frequency operation in the fiber laser. These two FBGs are designed so that only for one specific state of polarization the PM-FBG has a matched reflective wavelength with that of the non-PM FBG, thereby resulting in laser oscillation in this specific state of polarization. To achieve Q-switching in the fiber laser, an appropriate amount of pre-loaded stress is applied to a small section of the active fiber

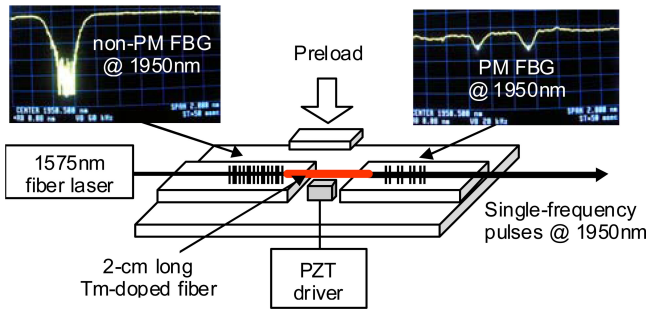

Fig. 10. A Q-switched Tm^{3+}-doped DBR fiber cavity was formed by two FBGs. Preload force and PZT-induced stress are applied to a small section of the active fiber for polarization modulation to achieve Q-switching. (Copied from [17]).

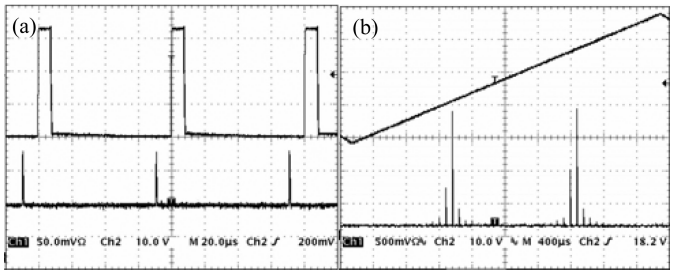

Fig. 11. (a) Q-switched pulse trains and their corresponding PZT drive signal at 12.5kHz. (b) Laser spectrum over one free spectral range of a scanning FP interferometer that verified single-frequency operation. (Copied from [17].)

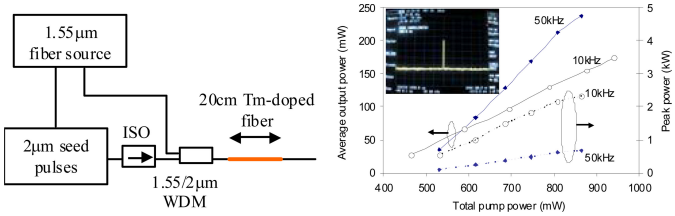

Fig. 12. A core-pumped fiber amplifier (left) can be used to boost the power of the single-frequency laser pulses (right). (Copied from [32].)

inside the laser cavity at an angle of 45 degree relative to the axes of the PM-FBG. This stress-induced birefringence acts as a wave-plate so that the intracavity light has the orthogonal direction of polarization with a low Q-value in the fiber laser cavity, thereby preventing from laser oscillation. A small piezo actuator can be used to quickly release the preload stress to obtain a high Q-value in the cavity, resulting in the generation of Q-switched single-frequency pulses in the preferred specific state of polarization.

Fig. 11 shows a typical Q-switched pulse train and their corresponding drive signal. Output power of the all-fiber Q-switched laser oscillator was about 10 mW. It can easily be increased by >10dB with a fiber amplifier core-pumped by a 1.55 μm fiber source, as shown in Fig. 12 [32].

B. Gain-Switched Single-Frequency Ho^{3+}*-Doped Fiber Laser*

A Ho^{3+}-doped fiber laser can be gain-switched by a Tm^{3+}-doped laser pulse near 1.95 μm. By doing this, we have demonstrated a gain-switched single-frequency Ho^{3+}-doped fiber laser

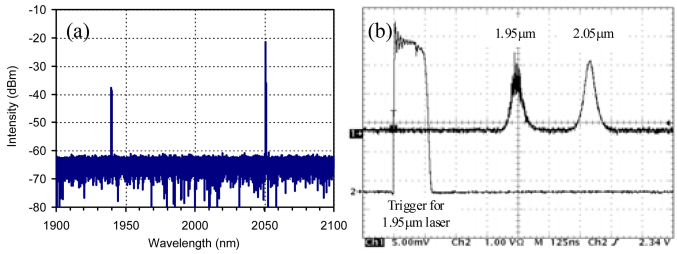

Fig. 13. (a) Optical spectrum and (b) temporal profile of the pump laser and the gain-switched laser. (Copied from [19].)

near the wavelength required for atmosphere Doppler LIDAR application, i.e., 2.05 μm [19].

An in-house Q-switched Tm-doped fiber laser was used as a pump source to pump a single-frequency Ho-doped fiber laser, which was formed by a 2-cm-long piece of the Ho-doped fiber and a pair of fiber Bragg gratings at 2.052 μm, including a high-reflectivity grating written in Corning SMF-28 fiber and an output coupler grating in polarization-maintaining fiber PM1550. The grating pair was designed for single polarization laser oscillation along the slow axis of the output grating, which emitted linearly polarized laser radiation with >20 dB polarization extinction ratio. The pump laser, i.e., single-mode Q-switched Tm-doped fiber laser, delivers 20 kHz pulses at 1.95 μm with a pulse width ranging from 15 to ~100 ns (inversely proportional to average output power approximately, with a maximum average power of about 300 mW).

Fig. 13 shows optical and temporal characteristics of the pump laser and the gain-switched laser. The gain-switched laser wavelength was measured to be 2.052 μm. The pump pulse and the gain-switched pulse were measured in time domain by using a fast photodiode and a digital oscilloscope. It can clearly be seen that the 1.95-μm pump pulse profile is spiky due to mode beating, but the gain-switched pulse at 2.052 μm has a very smooth profile, suggesting that the gain-switched fiber laser was in single-frequency laser operation. The single-frequency operation was verified by using a scanning fiber FP interferometer with a 1-GHz free-spectrum range (made by Micro-Optics). In the gain-switched mode, typical laser pulses have a transform-limited linewidth ranging from <10 MHz to ~40 MHz, depending on the pulsewidth of gain-switched pulses (which could be varied from less than 10 ns to more than 100 ns, as a function of pump power).

Output power of the single-frequency gain-switched laser was further boosted by a single-mode cladding-pumped fiber amplifier, in which the active fiber was 1.2-m-long piece of homemade Tm-Ho-codoped silicate glass fiber pumped by a multimode laser diode at 803 nm. The heavily codoped fiber has a 10-μm core diameter (0.14 NA) with 6-wt% Tm-doping and 0.4-wt% Ho-doping. The co-doped active fiber enables direct diode-pumping with 0.8-μm laser diodes. A 1-meter-long piece of passive fiber was spliced with the gain fiber to remove the residual pump from the fiber cladding and deliver the amplified single-mode gain-switched pulses at 2.052 μm. Fig. 13 shows the output power from the fiber amplifier as a function of pump power. The maximum extractable output power could reach 1.1 W at a pump power of 12 W with a slope efficiency of

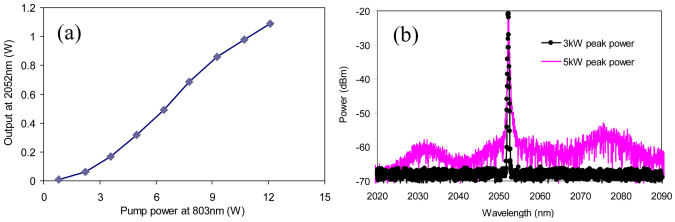

Fig. 14. (a) Output power and (b) optical spectra of the gain-switched laser pulses after a fiber amplifier. (Copied from [19].)

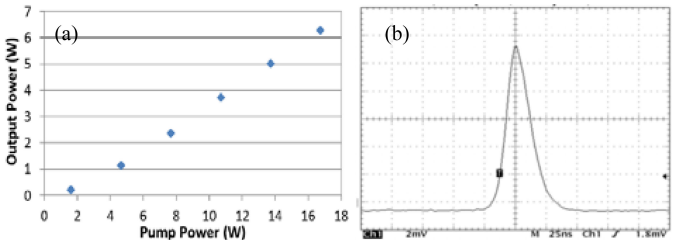

Fig. 15. (a) Output power as a function of absorbed pump power from the fiber system. (b) A typical temporal shape of an amplified pulse.

about 11%, corresponding to a maximum peak power of 7 kW approximately.

With 10-μm core fiber amplifier, experiments reveal that two different nonlinear effects are involved at a high peak power. One was four-wave mixing or modulation instability (MI). This kind of nonlinear effect was evidenced by the appearance of MI sidebands in the laser output spectra, as shown in the right graph of Fig. 14. At relatively low power ($\sim$500 mW average power or $\sim$3 kW peak power), no significant nonlinear effect was observed. But at higher pump power ($\sim$750 mW average power or $\sim$4.5 kW peak power), two symmetrical broad side-bands gradually grew up at both spectral sides of the laser line with 40 dB signal-to-noise (SN) ratio and 20 nm spectral spacing.

The other kind of nonlinear effect can also be seen when zooming in the spectra. Multiple spectral components appeared at the long wavelength side of the laser line when the peak power was over 4.5 kW. These red-shift spectral components were assigned as the Stokes components of stimulated Brillouin scattering. Obviously, the peak power ($\sim$4.5-kW) of the single-frequency laser pulses was too high for the 10-μm core fiber even at a fiber length of $\sim$2 m. To mitigate these two kinds of nonlinear effects, a simple solution is to use active fiber with larger core diameter for higher-power pulsed laser output.

C. *Power Scaling of* Tm^{3+}*-Doped Pulsed Fiber Laser*

We have further scaled up output power of the fiber laser pulses by used our large-mode-area heavily Tm^{3+}-doped silicate glass fiber in a power amplifier. The whole fiber amplifier system consists of a pulsed seed laser, fiber pre-amplifier, and a power amplifier. This preamplifier can increase the pulsed laser power from a few mW to well above 500 mW. The power amplifier included a 55-cm long piece of Tm^{3+}-doped gain fiber (20-μm core diameter and 0.08 NA). With the input of 20 μJ pre-amplified pulses (20 ns pulse width) at 10 kHz, the output characteristic of the power amplifier is shown in Fig. 15.

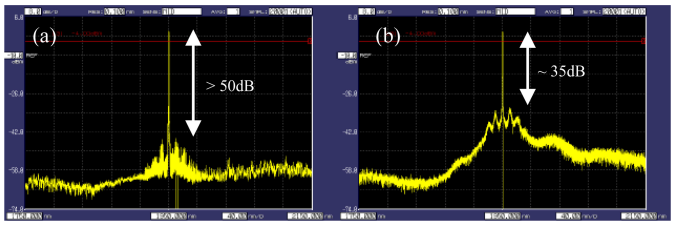

Fig. 16. Spectra of the laser pulses from the power amplifier at a pulse rate of (a) 20 kHz and (b) 10 kHz. The wavelength span is from 1750 nm to 2150 nm.

With 16-W absorbed pump power, the output spectra from the system at two different repetition rates were shown in Fig. 16. At 20 kHz or above, the SN ratio of the laser pulses was 50 dB or better. At 10 kHz, however, the SN ratio reduced to 35 dB, which accounts for about 5–10% noise in the total power at 10 kHz. The maximum pulse energy extracted from the 20-μm-core fiber power amplifier was $\sim$600 μJ with a peak power of about 30 kW.

VI. Mode-Locked Fiber Lasers Near 2 μm

Mode-locked fiber lasers at the 1-μm and 1.5-μm wavelength regions have been studied extensively in the last two decades. In the recent years, significant research efforts have been made for extending the mode-locking technology into a longer wavelength, particularly in the 2-μm spectral region. Broad gain bandwidth of both Tm^{3+}- and Ho^{3+}-doped silicate glass fibers makes them an appropriate gain medium for ultrashort pulse generation in the region.

Mode-locked fiber lasers can be designed for operation in several different regimes, including soliton, stretched-pulse, and all-normal-dispersion regime. Soliton mode-locking is most common for fiber lasers with relatively large anomalous cavity dispersion. Although soliton operation can generate clean pulse shape, the pulse energy and peak power are limited due to soliton effects. The group velocity dispersion (GVD) of the single-mode silica fiber at 2 μm is -0.065 ps^2/m, which is much larger than the GVD of -0.022 ps^2/m at 1.55 μm. Therefore most mode-locked Tm fiber lasers are soliton mode-locking with the pulse width limited to picoseconds or a few hundred of femtoseconds.

Silicate glass fibers have different characteristics of material dispersion from silica-based fibers. More importantly, because we use a rod-in-tube technique for fiber fabrication at a low cost, it is very flexible for us to design and fabricate silicate glass fibers with different waveguide dispersion to further modify overall fiber dispersion, in order to achieve different regimes of mode-locking operation. We have demonstrated soliton mode-locking laser operation with both Tm- and Ho-doped silicate fibers, and achieved $\sim$GHz high repetition rate mode-locked thulium fiber laser, stretched pulse mode-locking operation, and normal dispersion dominated mode-locking operation.

A. *Dispersion of Silicate Glasses and Fibers*

Sellmeier equation can be used to describe glass dispersion, i.e., $n^2 = 1 + \frac{B_1 l^2}{l^2 - C_1} + \frac{B_2 l^2}{l^2 - C_2} + \frac{B_3 l^2}{l^2 - C_3}$, where the wavelength λ is in the unit of μm. Prior to engineering zero dispersion wavelength (ZDW) of our own silicate glass fibers, we have

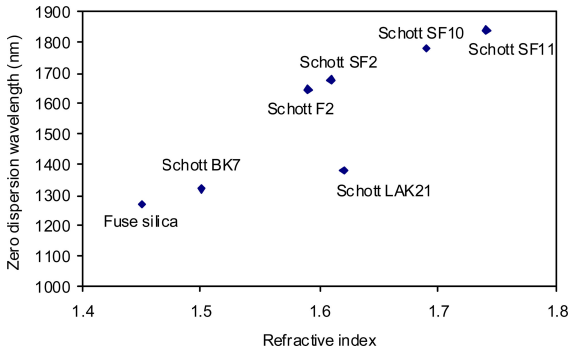

Fig. 17. ZDW versus refractive index for fuse silica and some Schott glasses.

TABLE I
DISPERSION OF IN-HOUSE SILICATE FIBER AT DIFFERENT WAVELENGTHS

λ (μm)	1.5	1.54	1.72	1.8	2.0
Slope (ps/nm)	-0.0217	-0.0175	0	0.0083	0.0283
Dispersion *(ps/km.nm)*	-18.08	-16.53	0	6.92	23.58

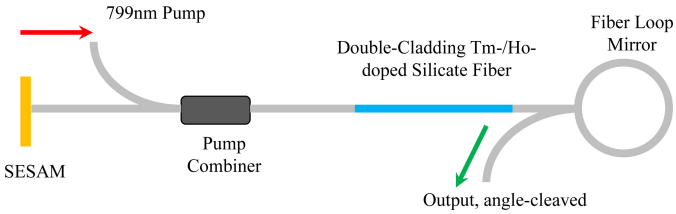

Fig. 18. Schematic of a mode-locked fiber laser with either Tm^{3+}-doped or $Tm^{3+}-Ho^{3+}$-codoped silicate fiber.

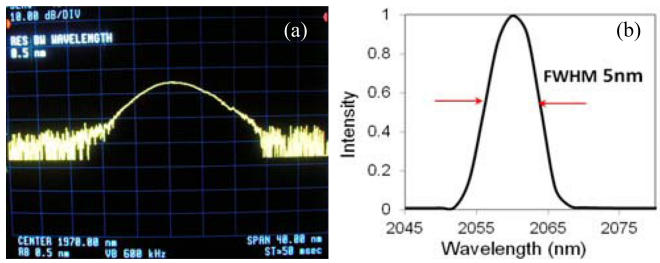

Fig. 19. Laser spectrum of a mode-locked silicate fiber laser. (a) 30-cm Tm^{3+}-doped silicate fiber. (b) 120-cm $Tm^{3+}-Ho^{3+}$-codoped silicate fiber.

investigated dispersion properties of some commercial glasses with the parameters published on-line [33].

With the published data, we are able to calculate ZDW of these commercial materials. Fig. 17 shows the ZDW of the glasses versus their refractive index. It is clear that these glasses have quite different refractive index (due to different glass composition) and different ZDW. Except for Schott LAK21 glass in Fig. 17, it is likely that glass ZDW increases with their refractive index. Since the silicate glass is a kind of multi-component glasses, we can easily engineer its glass composition to obtain different refractive index and material dispersion as well.

We have used standard white-light interferometry technique to characterize the dispersion of our own silicate fibers. As an example, Table I lists the result for one of single-mode silicate fibers. The ZDW of the fiber is around 1720 nm, and it exhibits weakly anomalous dispersion in the 2-μm spectral region. Our calculation indicates that after further introducing waveguide dispersion by using small-core fiber structure with high NA, the ZDW of our silicate glass fibers can be easily shifted to 2 μm spectral region or well beyond.

B. Soliton Pulses With Tm^{3+}- and Ho^{3+}-Doped Silicate Fiber

Soliton mode-locking has been demonstrated in a linear-cavity fiber laser with doped silicate glass fibers with an experimental setup shown in Fig. 18. The key element used to start and maintain mode-locking operation of the laser was a resonant Sb-based saturable absorber mirror. The linear laser cavity was formed by a SESAM, a pump combiner, a piece of double cladding Tm^{3+}-doped or Tm^{3+} -Ho^{3+}-codoped silicate fiber with 10 μm core diameter and a fiber loop mirror. The fiber loop mirror was a 50/50 fiber coupler, and it has an estimated reflectivity of $\sim 90\%$ at 2 μm. Due to the large difference in refractive index between passive silica fibers (pigtail fibers for the combiner and loop mirror) and our silicate active fiber, we angle-fusion-splice the two different kinds of fibers, so as to prevent from any spurious reflection that could be detrimental to mode-locking operation. The fiber output end was also angle-cleaved to eliminate back reflection. The input end of the pump combiner signal fiber was directly butt-coupled to the saturable absorber mirror.

We have demonstrated soliton mode-locking with both our Tm^{3+}-doped silicate fiber (with a length of 30 cm) [34] and Tm^{3+} -Ho^{3+}-codoped silicate fiber (with a length of 120 cm) [35]. Fig. 19 shows typical laser spectra of a mode-locked fiber laser with Tm^{3+}-doped silicate fiber (left graph) or $Tm^{3+}-Ho^{3+}$-codoped silicate fiber (right graph). With 30-cm Tm^{3+}-doped silicate fiber, central wavelength of the mode-locked pulses was around 1.97 μm with a full width half maximum (FWHM) of $\sim$7 nm. The pulse width was measured to be about 1.5 ps [34]. The time-bandwidth product was about 0.8, indicating chirping in laser pulses. With 120-cm Tm^{3+} -Ho^{3+}-codoped silicate fiber, the central wavelength of the mode-locked pulses was around 2.06 μm with a FWHM spectral bandwidth of $\sim$5 nm and a pulse width of 1.1 ps [35]. The time-bandwidth product was 0.38, indicating nearly transform-limited pulses at 2.06 μm.

C. GHz-Rate Mode-Locking Near 2 μm

High repetition rate mode-locking was also demonstrated in a Tm^{3+}-doped fiber laser. A short linear cavity with a short piece of Tm^{3+}-doped fiber core-pumped at 1.56 μm was used to achieve GHz-rate mode-locking. One end of the laser cavity was a SESAM mirror, and the other end was a fiber mirror with dielectric coating on the SMF-28 fiber end for anti-reflective at 1.55 μm and 80% reflectivity at 2 μm. The shortest laser cavity was about 10 cm. With this short cavity laser, we obtained mode-locking operation at a repetition rate of 982 MHz, which is, to our knowledge, the highest repetition rate of a mode-locked laser operating at 2 μm. Fig. 20 shows radio-frequency spectra of the laser in CW operation (left) and mode-locking operation

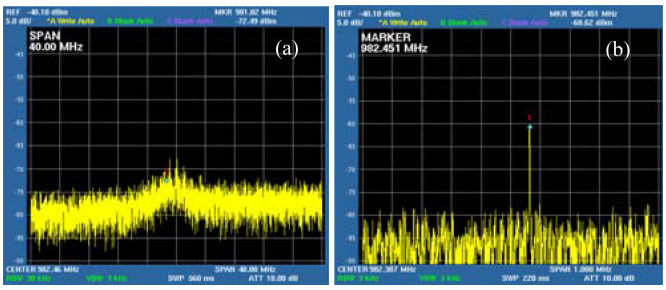

Fig. 20. Radio-frequency spectra of a Tm^{3+}-doped fiber laser in (a) CW operation and (b) mode-locking operation.

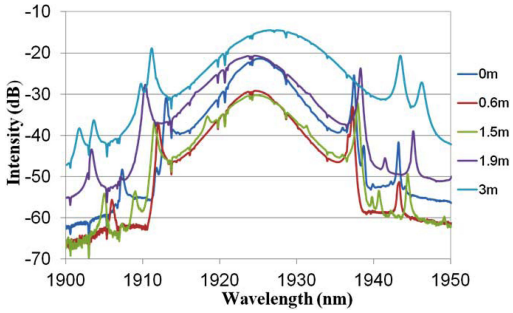

Fig. 21. Optical spectra of the stretched-pulse mode-locked fiber laser with different lengths of the normal dispersion fiber inserted in the laser cavity.

(right). The low signal to noise ratio of the spectra in Fig. 20 was due to the low sensitivity of the detector at the higher frequency.

D. Stretched-Pulse Mode-Locking

Typical spectral width (FWHM) of our Tm^{3+}-doped or Tm^{3+} -Ho^{3+}-codoped mode-locked silicate fiber laser was about 6 $\sim$ 7 nm, which is limited by large amount of anomalous dispersion in the cavity. In this case, the mode-locked laser operates in the soliton regime, which has limited pulse energy and peak power due to the soliton effect. In order to achieve broader laser spectrum and shorter pulse duration, the stretched-pulse mode-locking was studied in our 2-μm fiber lasers. By inserting a piece of 2-μm normal dispersion fiber, the total cavity dispersion was brought down to zero. As a result, the pump threshold for mode-locking operation slightly increased, and the mode-locked laser spectrum was significantly broadened. Fig. 21 shows the typical laser spectral at different lengths of the inserted normal dispersion fiber. The FWHM spectral bandwidth of the laser could be increased from 6 nm to 22 nm while the NDF length was increased (the total cavity dispersion was decreased). With 22-nm FWHM, the pulse width was measured to be 1.4 ps, indicating highly chirping of the output pulses. Less than 250 fs laser pulses could be expected after pulse compression.

E. Normal Dispersion Dominated Mode-Locking Regime

When the total cavity dispersion became positive, dissipative solitons were observed under appropriate pump power and cavity dispersion. The highly-chirped dissipative soliton pulses had pulse duration of about 724 fs. Using a piece of SMF-28 fiber as a pulse compressor, the pulses were compressed to 140 fs, as

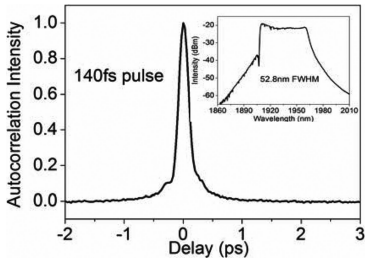

Fig. 22. Autocorrelation curve of a Tm^{3+}-doped mode-locked fiber laser in a normal dispersion dominated regime after pulse compression by using a piece of SMF28 fiber. Inset is the corresponding laser spectrum.

shown in Fig. 22. However, a significant change in spectral lineshape of the pulses was seen before and after pulse compression, which was attributed to nonlinear effects in the fiber compressor, such as SPM. The inset of Fig. 22 shows the laser spectrum after pulse compression. Considering the large bandwidth of the pulse spectrum, less than 100-fs pulses should be achieved if the nonlinear effects are eliminated by using an appropriate bulky grating pair.

F. Mode-Locking Fiber Amplifier

Our Tm^{3+}-doped silicate fibers have also been used to build fiber amplifiers to boost the energy of the mode-locked laser pulses. With a stretched-pulse mode-locked seed laser (0.3-nJ pulse energy), we obtained 20-nJ pulses with 16-kW peak power at a repetition rate of 34 MHz from a 10-μm fiber amplifier with a 30-cm-long Tm-doped silicate fiber. When using 22-μm-core and 0.06NA Tm^{3+}-doped silicate fiber with a length of 45 cm as the gain fiber (and 1.3-m delivery passive fiber), we obtained a maximum energy of 36-nJ mode-locked pulses with a measured pulse width of 1.1 ps, corresponding to $\sim$30-kW peak power.

VII. Conclusion

In summary, we have demonstrated various 2-μm fiber lasers by using our proprietary heavily Tm-doped and/or Ho-doped silicate fibers, including single-frequency fiber lasers, wavelength-swept fiber lasers, Q-switched nanosecond fiber lasers, picoseconds/femtosecond mode-locked fiber lasers operating in different regimes. The multi-components silicate glass fibers offer unique features as the gain fibers not only for various laser oscillators, but also for fiber amplifiers for their power scaling. These mid-infrared fiber lasers can be very useful light sources for many scientific and industrial applications.

References

[1] P. F. Moulton, G. A. Rines, E. V. Slobodtchikov, K. F. Wall, G. Frith, B. Samson, and A. L. G. Carter, "Tm-doped fiber lasers: Fundamentals and power scaling," *IEEE J. Select. Topics Quantum Electron.*, vol. 15, no. 1, pp. 85–92, Jan. 2009.

[2] S. W. Henderson, P. J. M. Suni, C. P. Hale, S. M. Hannon, J. R. Magee, D. L. Bruns, and E. H. Yuen, "Coherent laser radar at 2 μm using solid-state lasers," *IEEE Trans. Geosci. Remote Sens.*, vol. 31, no. 1, pp. 4–15, Jan. 1993.

[3] G. J. Koch, J. Y. Beyon, B. W. Barnes, M. Petro, J. Yu, F. Amzajerdian, M. J. Kavaya, and U. N. Singh, "High-energy 2 μm doppler lidar for wind measurements," *Opt. Eng.*, vol. 46, pp. 116201–116214, 2007.

[4] N. M. Fried, "Thulium fiber laser lithotripsy: An in vitro analysis of stone fragmentation using modulated 110-Watt thulium fiber laser at 1.94 μm," *Lasers Surg. Med.*, vol. 37, pp. 53–58, 2005.
[5] S. Chandra, M. E. Wager, B. Clayton, A. G. Geiser, T. H. Allik, J. L. Ahl, C. R. Miller, P. A. Budni, P. A. Ketteridge, K. G. Lanier, E. P. Chicklis, J. A. Hutchinson, and W. W. Hovis, "2 μm-pumped 8–12 μm OPO source for remote chemical sensing," *Proc. SPIE*, vol. 4036, pp. 200–208, 2000.
[6] G. Genty, S. Coen, and J. M. Dudley, "Fiber supercontinuum sources (Invited)," *J. Opt. Soc. Amer.*, vol. B24, pp. 1771–1785, 2007.
[7] J. Price, T. M. Monro, H. Ebendorff-Heidepriem, F. Poletti, P. Horak, V. Finazzi, J. Leong, P. Petropoulos, J. C. Flanagan, G. Brambilla, X. Feng, and D. J. Richardson, "Mid-IR supercontinuum generation from nonsilica microstructured optical fibers," *IEEE J. Select. Topics Quantum Electron.*, vol. 13, no. 3, pp. 738–749, May/Jun. 2007.
[8] J. Geng, Q. Wang, and S. Jiang, "2 μm fiber laser sources and their applications," *Proc. SPIE*, vol. 8164, pp. 816409-1–816409-10, 2011.
[9] J. Wu, S. Jiang, T. Luo, J. Geng, N. Peyghambarian, and N. P. Barnes, "Efficient thulium-doped 2-μm germanate fiber laser," *IEEE Photon. Technol. Lett.*, vol. 18, no. 2, pp. 334–336, Jan. 2006.
[10] J. Wu, S. Jiang, T. Qui, M. Kuwata-Gonokami, and N. Peyghambarian, "2 μm lasing from highly thulium doped tellurite glass microsphere," *App. Phys. Lett.*, vol. 87, pp. 211118–211120, 2005.
[11] M. Gorjan, T. North, and M. Rochette, "Model of the amplified spontaneous emission generation in thulium-doped silica fibers," *J. Opt. Soc. Amer.*, vol. B29, pp. 2886–2890, 2012.
[12] S. Agger, J. H. Povlsen, and P. Varming, "Single-frequency thulium-doped distributed-feedback fiber laser," *Opt. Lett.*, vol. 29, pp. 1503–1505, 2004.
[13] N. Y. Voo, J. K. Sahu, and M. Ibsen, "345-mW 1836-nm single-frequency DFB fiber laser MOPA," *IEEE J. Photon. Technol. Lett.*, vol. 17, no. 12, pp. 2550–2552, Dec. 2005.
[14] D. Gapontsev, N. Platonov, M. Meleshkevich, O. Mishechkin, O. Shkurikhin, S. Agger, P. Varming, and J. H. Poylsen, "20 W single-frequency fiber laser operating at 1.93 μm," presented at the Conf. Lasers Electro-Opt., Baltimore, MD, USA, May 6–11 2007, paper CFI5.
[15] Z. Zhang, D. Y. Shen, A. J. Boyland, J. K. Sahu, W. A. Clarkson, and M Ibsen, "High-power Tm-doped fiber distributed-feedback laser at 1943nm," *Opt. Lett.*, vol. 33, pp. 2059–2061, 2008.
[16] J. Geng, J. Wu, S. Jiang, and J. Yu, "Efficient operation of diode-pumped single-frequency thulium-doped fiber lasers near 2 μm," *Opt. Lett.*, vol. 32, pp. 355–357, 2007.
[17] J. Geng, Q. Wang, J. Smith, T. Luo, F. Amzajerdian, and S. Jiang, "All-fiber Q-switched single-frequency Tm-doped laser near 2 μm," *Opt. Lett.*, vol. 34, no. 23, pp. 3713–3715, 2009.
[18] J. Wu, Z. Yao, J. Zong, A. Chavez-Pirson, N. Peyghambarian, and J. Yu, "Single frequency fiber laser at 2.05 μm based on Ho-doped germinate glass fiber," *Proc. SPIE*, vol. 7195, pp. 71951K-1–71951K-7, 2009.
[19] J. Geng, Q. Wang, T. Luo, B. Case, S. Jiang, F. Amzajerdian, and J. Yu, "Single-frequency gain-switched Ho-doped fiber laser," *Opt. Lett.*, vol. 37, no. 18, pp. 3795–3797, 2012.
[20] D. C. Hanna, R. M. Percival, R. G. Smart, and A. C. Tropper, "Efficient and tunable operation of a Tm-doped fiber laser," *Opt. Commun.*, vol. 75, pp. 283–286, 1990.
[21] T. Haber, K. Hsu, C. M. Miller, and Y. Bao, "Tunable erbium-doped fiber ring laser precisely locked to the 50GHz ITU frequency grid," *IEEE Photon. Technol. Lett.*, vol. 12, no. 11, pp. 1456–1458, Nov. 2000.
[22] F. D. Nielsen, L. Thrane, J. Black, K. Hsu, A. O. Bjarklev, and P. E. Anderson, "Swept-wavelength source for optical coherence tomography in the 1 μm range," *Proc. SPIE*, vol. 5861, pp. 98–105, 2005.
[23] J. Geng, Q. Wang, J. Wang, S. Jiang, and K. Hsu, "All-fiber wavelength-swept laser near 2 μm," *Opt. Lett.*, vol. 36, no. 12, pp. 2293–2295, 2011.
[24] A. F. El-Sherif and T. A. King, "High-peak-power operation of a Q-switched Tm^{3+}-doped silica fiber laser operating near 2 μm," *Opt. Lett.*, vol. 28, pp. 22–24, 2003.
[25] J. Sahu, V. Philippov, J. Kim, C. Codemard, P. Dupriez, J. Nilsson, A. Abdolvand, and N. V. Kuleshov, "Passively Q-switched thulium-doped silica fiber laser," presented at the Conf. Lasers and Electro-Opt., San Francisco, CA, USA, 2004, paper CThGG7.
[26] S. D. Jackson, "Passively Q-switched Tm^{3+}-doped silica fiber lasers," *Appl. Opt.*, vol. 46, pp. 3311–3317, 2007.
[27] S. Kivisto, T. Hakulinen, M. Guina, K. Rößner, A. Forchel, and O. Okhotnikov, "2 Watt 2 μm Tm/Ho fiber laser system passively Q-switched by antimonide semiconductor saturable absorber," *Proc. SPIE*, vol. 6998, pp. 69980Q1–69980Q8, 2008.
[28] M. Jiang and P. Tayebati, "Stable 10ns, kilowatt peak-power pulse generation from a gain-switched Tm-doped fiber laser," *Opt. Lett.*, vol. 32, pp. 1797–1799, 2007.
[29] Y. Tang, L. Xu, Y. Yang, and J. Xu, "High-power gain-switched Tm^{3+}-doped fiber laser," *Opt. Exp.*, vol. 18, pp. 22964–22972, 2010.
[30] Y. Kaneda, C. Spiegelberg, J. Geng, and Y. Hu, "All-fiber Q-switched laser," U.S. Patent 7 130 319, 2006.
[31] J. Geng, Q. Wang, T. Luo, S. Jiang, and F. Amzajerdian, "Single-frequency narrow-linewidth Tm-doped fiber laser using silicate glass fiber," *Opt. Lett.*, vol. 34, no. 22, pp. 3493–3496, 2009.
[32] J. Geng, Q. Wang, Z. Jiang, T. Luo, S. Jiang, and G. Czarnecki, "Kilowatt-peak-power single-frequency pulsed fiber laser near 2 μm," *Opt. Lett.*, vol. 36, no. 12, pp. 2293–2295, 2011.
[33] (2011). http://www.cvimellesgriot.com/products/Documents/Catalog/Dispersion_Equations.pdf
[34] Q. Wang, J. Geng, T. Luo, and S. Jiang, "Mode-locked 2 μm laser with highly thulium-doped silicate fiber," *Opt. Lett.*, vol. 34, no. 23, pp. 3616–3618, 2009.
[35] Q. Wang, J. Geng, Z. Jiang, T. Luo, and S. Jiang, "Mode-locked Tm-Ho-codoped fiber laser at 2.06 μm," *IEEE Photon. Technol. Lett.*, vol. 23, no. 11, pp. 682–684, Jun. 2011.

Jihong Geng received the Ph.D. degree in optical science from the Shanghai Institue of Optics and Fine Mecahnics, Chinese Academy of Science, China. He is a Chief Scientist at AdValue Photonics, working on research and development of all kinds of 2 μm fiber laser product in the company, including single-frequency Tm- and Ho-doped fiber lasers, Q-switched and mode-locked 2 μm fiber lasers and amplifiers, mid-infrared supercontinuum lasers, and all-fiber isolators. He has more than 20-year experience in laser development for various industrial and scientific applications, including laser material processing, fiber optic sensing, optical communications, optical metrology, trace gas monitoring, and laser spectroscopy. Before joining AdValue Photonics, he held the positions as a Senior Staff Engineer at Spectra-Physics/Newport and a Senior Scientist at NP Photonics, developing various fiber lasers/amplifiers such as high-power picosecond Yb-doped fiber infrared/UV laser system, low-noise single-frequency fiber lasers at 1, 1.55, and 2 μm, ultranarrow-linewidth Brillouin fiber laser, and Brillouin fiber sensor system. From 1995 to 1999, he was a Frontier Researcher at the Institute of Physical and Chemical Research, Japan, working on high-resolution molecular spectroscopy by four-wave mixing, and development of electronically-tuned Ti:sapphire lasers. He has authored 50 publications, and more than ten awarded U.S. patents.

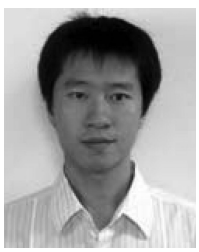

Qing Wang received the B.S. degree in optoelectronics in 2000 and the M.S. degree in physical electronics in 2003 from the Beijing Institute of Technology, Beijing, China. In 2005 and 2008, he received the M.S. and Ph.D. degrees in optical sciences from the University of Arizona, Tucson, USA. From 2003 to 2008, he was a Research Assistant with the University of Arizona. Since 2009, he has been a Senior Optical Scientist in AdValue Photonics Inc., Tucson, Arizona. He has authored about 20 articles. He has more than ten years research experiences in various fiber lasers, waveguide lasers, and solid state lasers. He has been actively conducting research and development on rare-earth-doped fiber lasers, including CW, Q-switched, mode-locked and single-frequency lasers.

Yinwen Lee received the M.S. degree in electrical engineering from National Tsinghua University, and the Ph.D. degree in applied physics from Stanford University, Stanford, CA, USA, in 2000 and 2008, respectively. Her doctoral research centered on high-power fiber lasers and amplifiers, with special focus on power scaling capabilities of Yb^{3+}-doped phosphate fibers. From 2008 to 2010, she was a Postdoctoral Research Scientist in OFS Labs., where she was engaged in developing state-of-the-art kW-class fiber amplifiers and Raman fiber lasers. After the Postdoctoral Research at National Taiwan University, where she worked on development of pulse Yb^{3+}-doped fiber laser sources for efficient EUV generation, she joined the Electric-Optic Engineering Department at National Taipei University of Technology as an Assistant Professor in 2012. Her current research interests include investigating advanced fiber laser dopants and glass hosts to extend the accessible wavelength range of ultrafast fiber lasers as well as developing advanced Yb^{3+}-doped fiber laser systems for the applications in material processing, medical surgery instruments, and environmental/gas sensing.

Shibin Jiang received the B.S. degree from Zhejiang University, M.S. degree from the Shanghai Institute of Optics and Fine Mechanics, Chinese Academy of Sciences, and the Ph.D. degree in chemistry from the Universite de Rennes I, Rennes, France in 1996. He currently is President and CEO of AdValue Photonics Inc. and Adjunct Research Professor at College of Optical Sciences, University of Arizona. From 1996 to 2000, he was the Assistant Research Professor at the College of Optical Sciences, University of Arizona. During his stay at the University of Arizona, he established the Glass for Photonics Lab. From 2001 to 2008, he was co-founder and Chief Technology Officer of NP Photonics Inc. where he led the development of compact fiber amplifiers, single frequency fiber lasers, Brillouin fiber lasers, THz generations, as well as fiber sensing systems. He founded AdValue Photonics Inc in June 2007, where he focuses on his research on fiber lasers and amplifiers using rare-earth-doped multi-component glass fibers. He leaded the development of 2 μm single frequency fiber lasers, 2 μm Q-switched fiber lasers, 2 μm mode-locked fiber lasers, as well as all-fiber isolator at 1 μm wavelength. He has authored and co-authored more than 150 publications, edited 17 proceeding books, and holds 34 issued US patents. He has served as chair and co-chair of 21 technical conferences. He served as Associate Editor of the JOURNAL OF LIGHTWAVE TECHNOLOGY, and serves as Topic Editor of *Applied Optics*, Editorial Board of *Fiber and Integrated Optics* and *Chinese Optics Letters*.

Dr. Jiang was awarded with the Gottardi Prize in 2005 from International Commission on Glass (ICG) and R&D 100 Award in 2012. He is a Fellow of SPIE, the America Ceramic Society, and the Optical Society of America.